

**PROCEEDINGS  
NINTH WORKSHOP  
GEOTHERMAL RESERVOIR ENGINEERING**

**December 13-15, 1983**



**Henry J. Ramey, Jr., Paul Kruger, Frank G. Miller,  
Roland N. Horne, William E. Brigham,  
and Jon S. Gudmundsson  
Stanford Geothermal Program  
Workshop Report SGP-TR-74\***

## **DISCLAIMER**

**This report was prepared as an account of work sponsored by an agency of the United States Government. Neither the United States Government nor any agency Thereof, nor any of their employees, makes any warranty, express or implied, or assumes any legal liability or responsibility for the accuracy, completeness, or usefulness of any information, apparatus, product, or process disclosed, or represents that its use would not infringe privately owned rights. Reference herein to any specific commercial product, process, or service by trade name, trademark, manufacturer, or otherwise does not necessarily constitute or imply its endorsement, recommendation, or favoring by the United States Government or any agency thereof. The views and opinions of authors expressed herein do not necessarily state or reflect those of the United States Government or any agency thereof.**

## **DISCLAIMER**

**Portions of this document may be illegible in electronic image products. Images are produced from the best available original document.**

## VARIATION OF FRACTURING PRESSURES WITH DEPTH NEAR THE VALLES CALDERA

Zora Dash and Hugh Murphy

Los Alamos National Laboratory, MS J981  
Los Alamos, New Mexico 87545

### ABSTRACT

Hydraulic Fracturing at the Fenton Hill Hot Dry Rock Geothermal site near the Valles Caldera has yielded fracturing pressures from 14 to 81 MPa (2030 to 11750 psi) at depths ranging from 0.7 to 4.4 km (2250 to 14400 ft). This data can be fit to a fracture gradient of 19 MPa/km (0.84 psi/ft), except for an anomalous region between 2.6 to 3.2 km where fracturing pressures are about 20 MPa lower than estimated using the above gradient. This anomaly coincides with a biotite granodiorite intrusive emplaced into a heterogeneous jointed metamorphic complex comprised of gneisses, schists and metavolcanic rocks. Microseismic events detected with sensitive downhole geophones suggest that shear failure is an important process during hydraulic fracturing of such jointed rock. Consequently the usual relation between minimum earth stress and fracture opening pressure, based upon classic tensile failure, cannot be used a priori; fracture opening pressure is instead a complex function of joint orientation and all three components of principal earth stress.

### FRACTURING EXPERIMENTS

The Los Alamos National Laboratory, with financial support from the U.S. D.O.E., West Germany's Ministry for Science and Technology, and Japan's New Energy Development Organization, has drilled five wells into Precambrian crystalline basement rock as part of the Hot Dry Rock geothermal energy program. The experimental site, Fenton Hill, is located in the western flank of the Valles Caldera, a dormant volcano in the Jemez Mountains of northern New Mexico. The first well, GT-1, was drilled to 0.75 km for exploratory purposes. The second and third wells, GT-2 and EE-1, were drilled to approximately 3 km, and were used for numerous HDR heat extraction experiments.<sup>1</sup> These wells were connected by hydraulic fractures, one of which extended vertically 300 m from initiation point in EE-1 to intersection with GT-2. The fourth and fifth wells, EE-2 and EE-3, were drilled to 4.4 and 4.0 km respectively. The temperature at 4.4 km was 325°C. The bottom sections of these wells were directionally drilled, at an angle of 35° from vertical, with horizontal

deviation in the ENE direction, parallel to the estimated direction of the minimum principal earth stress. These wells are to be connected by fractures which must be about 370 m high, because the wells are separated vertically by this distance.

In all fracturing experiments conducted to date, the fracturing fluid has been water, to which friction reducer and fine silica have been added occasionally to reduce wellbore friction and to increase fracturing efficiency by blocking permeability of the rock faces contiguous to the fracture. Other than the addition of friction reducer the water was not viscosified, and no proppants were injected. Injection rates have ranged from 1 to 76 l/s, and injection volumes from 1 to 5000 m<sup>3</sup>. The great depths and temperatures have so far precluded the successful use of impression packers or televiwers to determine fracture orientation, but monitoring of microseismic acoustic emissions during fracturing with 3 axis geophones installed to depths of 2.9 km in neighboring wells indicate that the fracture planes generally strike NS, nearly as expected. All fractures are vertical, or nearly so, except in the lower zone of EE-2, (below 4.3 km) where acoustic emission patterns suggest a fracture zone with a dip of 45°.

Table I summarizes total downhole fracture pressures,  $P_f$ , determined in all fracture experiments conducted in the Fenton Hill geothermal wells to date. Later we discuss the relationship of  $P_f$  and minimum horizontal earth stress. The designation ISIP indicates that a reasonably constant pressure was observed after shut-in, but extrapolated ISIP indicates that the "Muskat analysis" was required, in which a straight line fit of logarithm of pressure versus time is extrapolated back to actual time of shut-in.<sup>2</sup> "Fracture extension" indicates that re-injection provided such a clear arrest in the pressure-time curve, and at reasonably low flow rates, that this arrest could be taken as  $P_f$ . The designation "P from PTA" indicates the fracture extension pressure derived from noting the pressure required to change hydrological characteristics of the existing fracture, e.g. enlargement. The last two methods of  $P_f$  determination, termed P vs Q<sup>0.25</sup>

Table I. Fenton Hill Fracture Pressures			
Well / Expt	Depth (km)	Fracture Opening Pressure (MPa)	Method Of Determination
<u>GT-1</u>	0.745	13.7-14.8	ISIP
<u>GT-2</u>	2.0	33.5-34.9	Extrapolated ISIP
	2.93	36.6-37.3	Fracture Extension
<u>EE-1</u>	1.96	30.6-31.5	Fracture Extension
	2.93	37.5	Fracture extension pressure from PTA
<u>EE-2</u> 2018(82/07/19)	3.46-3.59	61.0(6)*	P vs Q <sup>0.25</sup> Extrapolation
		67.5(6)	P vs Q <sup>0.5</sup> Extrapolation
2020(82/10/06)	3.46-3.59	62.7	ISIP
		75.0	Extrapolated ISIP
2020(82/10/06)	3.46-3.59	63.0(5)	P vs Q <sup>0.25</sup> Extrapolation
		68.5(5)	P vs Q <sup>0.5</sup> Extrapolation
2011(82/05/30)	4.25-4.36	67.7-73.9	ISIP (4 measurements)
		70.0-74.2	Extrapolated ISIP (3)
2011(82/05/30)	4.25-4.36	59.2(2)	P vs Q <sup>0.25</sup> Extrapolation
		69.9(2)	P vs Q <sup>0.5</sup> Extrapolation
2012(82/06/04)	4.25-4.36	80.2	ISIP
		80.3	Extrapolated ISIP
2012(82/06/04)	4.25-4.36	74.5(7)	P vs Q <sup>0.25</sup> Extrapolation
		78.7(7)	P vs Q <sup>0.5</sup> Extrapolation
2016(82/06/19)	4.25-4.36	80.2	ISIP
		80.3	Extrapolated ISIP
2016(82/06/19)	4.25-4.36	71.7(9)	P vs Q <sup>0.25</sup> Extrapolation
		77.0(9)	P vs Q <sup>0.5</sup> Extrapolation
<u>EE-3</u> 2006(82/01/19)	3.09-3.15	81.2	ISIP
		81.3	Extrapolated ISIP
2006(82/01/19)	3.09-3.15	38.1	Extrapolated ISIP
2007(82/02/17)	3.09-3.15	33.6(3)	P vs Q <sup>0.25</sup> Extrapolation
		35.9(3)	P vs Q <sup>0.5</sup> Extrapolation
2023(82/11/08)	3.09-3.15	38.4	Extrapolated ISIP
2023(82/11/08)	3.09-3.15	33.9(6)	P vs Q <sup>0.25</sup> Extrapolation
		37.3(6)	P vs Q <sup>0.5</sup> Extrapolation
2025(82/12/14)	3.35-3.44	38.6	ISIP
		42.5	Extrapolated ISIP
2025(82/12/14)	3.35-3.44	45.4(14)	P vs Q <sup>0.25</sup> Extrapolation
		56.6(14)	P vs Q <sup>0.5</sup> Extrapolation

\* Number in Parentheses is Number of P - Q Data Points in Curve Fit.

(laminar flow) and  $P$  vs  $Q^{0.5}$  (turbulent flow) are scaling laws for refracturing pressure variation with flow rate, using a simple fracture aperture (opening) and pressure relation<sup>3</sup>. Figure 1 presents the variation of the fracture extension pressure with  $Q$  for Experiment 2012. As can be seen, reasonable fits to the data can be obtained with either  $Q^{0.25}$  or  $Q^{0.5}$  scaling, a typical value of the discrepancy between data and curve fit being only about 1%. The values of  $P_f$  obtained by extrapolation are 74.5 MPa for  $Q^{0.25}$  scaling and 78.7 MPa for  $Q^{0.5}$  scaling, but below we show that this difference, though small, is significant and we will argue that  $Q^{0.5}$  scaling is more appropriate.

The single value of  $P_f$  derived from PTA was based upon 15 injection tests.<sup>4</sup> The range of ISIPs provided for Experiment 2020 represents four separate determinations<sup>5</sup> during the course of injecting 3300 m<sup>3</sup> (860,000 gallons) over 15 hours.

Table I demonstrates the excellent repeatability of all the methods of estimating  $P_f$ . For example, three separate fracturing experiments were conducted in EE-2 in the depth interval 4.25 to 4.36 km. The six separate  $P_f$  measurements by ISIP and extrapolated ISIP vary by a maximum of 1.4% from minimum to maximum.

For Experiment 2011, only two data points were available for  $P - Q$  curve fitting and, as can be seen, the value of  $P_f$  so derived is significantly different from the other estimates. For the other two experiments at 4.25 to 4.36 km, the number of data points was greater and the agreement is much better. In fact, if the  $P_f$  estimates based upon two point  $P$  vs  $Q$  extrapolation are excluded, the agreement of the remaining  $P_f$  estimates is excellent, ranging only from 71.7 to 81.3 MPa, or a variation of 6% about the mean. Similar observations pertain for the 8 measurements of  $P_f$  at 3.46 to 3.59 km in EE-2 and the 8 measurements at about 3.1 km in EE-3.

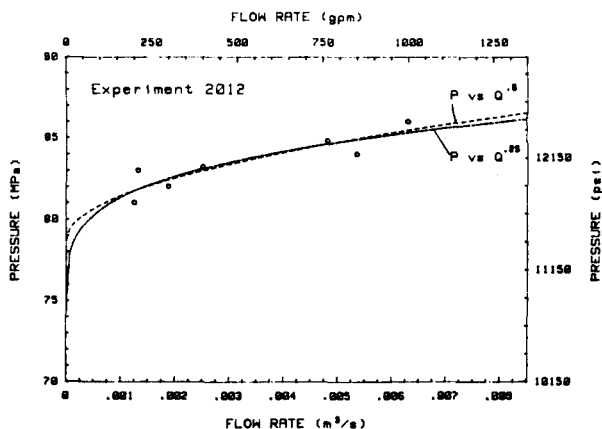


Figure 1. Variation of fracture extension pressure with injection rate.

With the possible exception of Experiment 2018, the  $P_f$  determined from  $Q^{0.25}$  extrapolation is always significantly lower than the other determinations. This argues that a laminar flow rule is inappropriate, an entirely reasonable finding considering the high injection rates used in these experiments. If  $Q^{0.25}$  extrapolation is excluded from consideration, the agreement of  $P_f$  determinations would be  $\pm 3\%$  at 4.3 km,  $\pm 8\%$  at 3.5 km, and  $\pm 8\%$  at 3.1 km.

Figure 2 presents the variation of fracture pressure with depth. All measurements, with the exception of those from  $P - Q^{0.25}$  extrapolation and the two-point  $Q$  extrapolation are plotted. Also shown is the vertical overburden stress computed from the density of the overlying formations. Except for the biotite granodiorite intrusive located at 2.6 to 3.2 km,  $P_f$  can be represented as a linear function of depth, with a fracture pressure gradient of 19 MPa/km (0.84 psi/foot).

#### RELATIONSHIP OF FRACTURE PRESSURE AND EARTH STRESSES

According to conventional theory, the fracture pressure derived from shut-in or from fracture extension pressure is equivalent to the minimum principal earth stress,  $S_{min}$ . However, before this equivalence can be drawn for the present measurements it must be shown that the mode of fracturing is tensile in nature, not due to shear. In addition, because

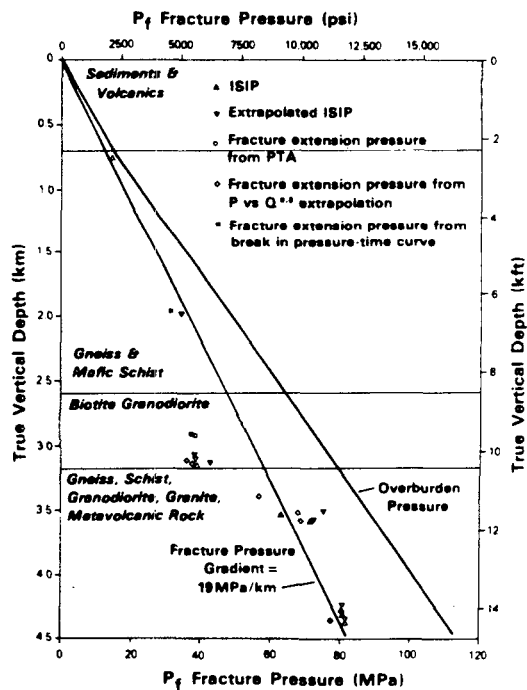


Figure 2. Variation of fracture pressure with depth.

fracturing in these crystalline rock formations undoubtedly opens up pre-existing fractures, or joints, rather than creating virgin rock failures, it must also be shown that the joints preferentially stimulated are perpendicular, or nearly so, to  $S_{min}$ , or else that the principal earth stresses are sufficiently close in magnitude that joint orientation makes little difference. Let us first consider the possibility of shear fracturing. For joints without strength or cohesion, it can be shown that as the fluid pressure is increased, eventually the effective normal stress on the joint will be reduced to the point where the joint can slip; theoretically shear slippage occurs before the effective stress is reduced to zero, and the joint completely opens ("jacking" is the descriptive term used in reference 6). Adopting Amonton's friction law, it can be shown that if  $\beta$  is the angle between a joint plane and the direction of the maximum principal stress,  $S_{max}$ , and  $\phi$  is the friction angle, (the coefficient of friction is  $\tan \phi$ ) then

$$\frac{S_{min}}{P_f} = \frac{2 + (\lambda - 1) S_{max}/P_f}{\lambda + 1} \quad (1)$$

where  $\lambda = \cos 2\beta + (\sin 2\beta)/\tan \phi$ .

Thus  $S_{min}$  can be estimated from the measured  $P_f$  if independent estimates of  $S_{max}$ ,  $\beta$  and  $\phi$  are available. Usually  $S_{max}$  is the readily estimated overburden stress, but in tectonically active regions such as the Valles Caldera this must be established, and the means of doing so was derived from differential strain analysis (DSA) of core specimens<sup>8</sup> as well as fault plane solutions<sup>9</sup> of microseismic acoustic emissions. DSA earth stress measurements are based upon the stress required to close microcracks in the core, the assumption being that all such cracks are closed *in situ*. This method is consequently qualitative in nature, subject to considerable uncertainties, and with a tendency to overestimate actual earth stress. Figure 3 presents the results: the solid lines indicate the estimated minimum horizontal stresses, and the dashed lines represent the maximum horizontal stresses. The four core specimens were unoriented, so the direction of the DSA principal horizontal stresses are unknown. While considerable uncertainty is noted it appears that the maximum horizontal stress is less than, or approximately equal to, the vertical stress.

Microseismic acoustic emissions during hydraulic fracturing experiments were detected with a downhole, three-axis geophone (or occasionally an accelerometer) as well as a surface network of 13 stations located within 5 km of the geothermal wells. Full details are provided in reference 9, but can be summarized as follows: the fault plane solution for fracturing at the 4.3 km interval

in EE-2 indicates strike slip faulting on a N-S vertical plane. The solution at 3.5 km indicates dip slip on a N-S vertical plane. These two solutions indicate that over a short depth interval, only 800 m, the maximum earth stress changes from nearly vertical to nearly horizontal, which strongly implies that the maximum horizontal stress is nearly equal to the overburden stress over this depth interval, being slightly greater at 3.5 km, and slightly less at 4.3 km. This result is entirely consistent with the DSA stress ranges shown in Figure 3. Consequently the magnitude of the maximum stress can be taken as that of the overburden stress. At 3.5 km the ratio  $S/P_f$  is then 1.30 while at 4.3 km the ratio is 1.37; both intervals can be characterized, on average, as  $S_{max}/P_f = 1.34$ . Substitution in equation (1) yields, in Table II, the ratios of  $S_{min}/P_f$  provided by the shearing criterion for various values of fracture orientation and friction angle. Friction angles of  $30^\circ$  to  $60^\circ$  encompass the range of reasonable values for crystalline granitic rock.

For the 3.5 km interval the fault plane was not well constrained, and the plane could dip from  $50^\circ$  to  $90^\circ$  ( $\beta = 0^\circ$  to  $40^\circ$ ). The fracture orientation provided by mapping the microseismic hypocenters is also poorly constrained, but the general pattern appears to be a vertical fracture striking roughly N-S. The fault plane solution for the 4.3 km interval is more tightly constrained, with dip of  $85^\circ$  and strike  $N10^\circ E$ . Usual fault plane convention places the P axis direction at  $45^\circ$  to the fault, so  $\beta = 45^\circ$ . However, hypocenter maps suggest a fracture dipping  $45^\circ$  and striking roughly N-S. This could be construed as a single fracture, with a dip at variance with that given by the fault plane solution (but still with  $\beta \leq 45^\circ$ ), or as a series of en echelon fractures, each with vertical fault plane, but joined to adjacent fractures by off-vertical natural joints.

In every case discussed,  $\beta < 45^\circ$ , so that the minimum earth stresses in Table II are remarkably well constrained:  $S_{min}/P_f = 1.08 \pm 8\%$ , for  $30^\circ < \phi < 60^\circ$ . Thus the use of either the conventional interpretation or one

Table II  
Ratios of Minimum Earth Stress To Fracture Pressure According to Shear Fracturing Criterion With  $S_{max}/P_f = 1.34$ .

$\beta$	$\phi = 30^\circ$	$\phi = 45^\circ$	$\phi = 60^\circ$
$0^\circ$	1.00	1.00	1.00
$15^\circ$	1.09	1.05	1.02
$30^\circ$	1.17	1.05	1.00
$45^\circ$	1.07	1.00	0.91
$60^\circ$	1.00	0.84	0.64
$75^\circ$	0.66	0.27	-0.26

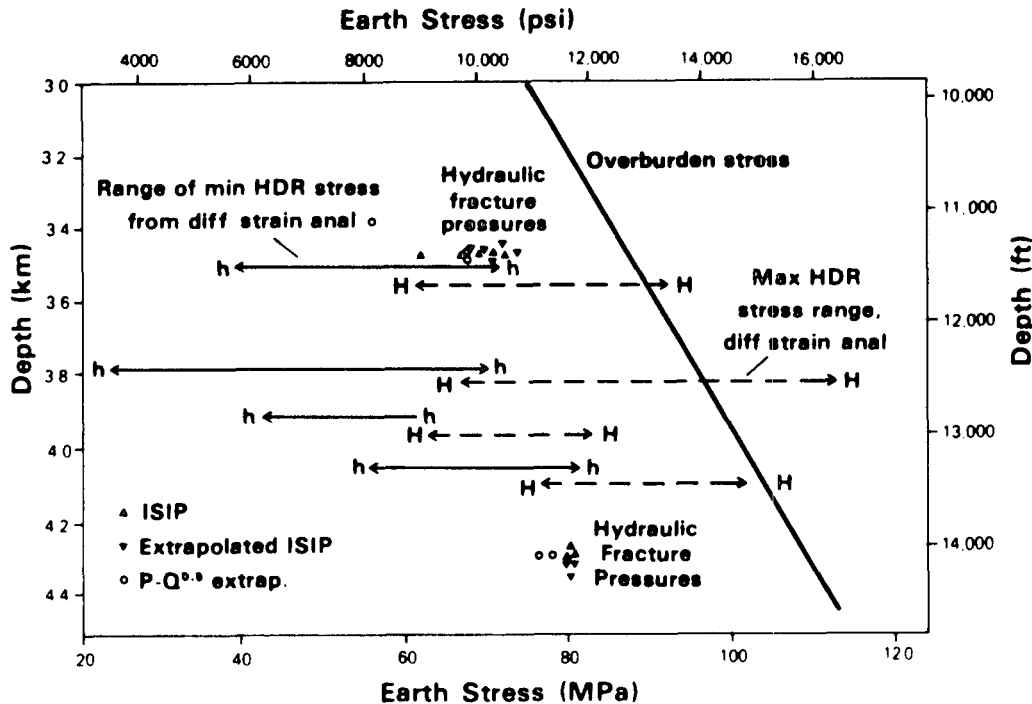


Figure 3. Comparison of DSA Earth Stresses and Fracture Pressures.

based upon shear fracturing results in essentially the same result,  $S_{min} = P_f$ , or  $S_{min} = 1.08 (\pm 0.08) P_f$ .

The final check is to consider the possibility of joint "jacking" on planes non-perpendicular to  $S_{min}$ . In this case the normal stress must be equal to  $P_f$ , and rotational stress transformation yields:

$$\frac{S_{min}}{P_f} = \frac{2 - (1 - \cos 2\beta) S_{max}/P_f}{1 + \cos 2\beta} \quad (2)$$

Table III indicates that unlike shear fracturing, it requires a fracture pressure greater than  $S_{min}$  to jack open joints inclined significantly to the  $S_{max}$  direction. It may be concluded that static considerations alone preclude the opening of such off angle joints by jacking, because these would shear first.

Table III

Ratio of Minimum Earth Stress To Fracture Pressure For "Jacking";  $S_{max}/P_f = 1.34$

$\beta$	$S_{min}/P_f$
0°	1
15°	0.97
30°	0.89
45°	0.66

However dynamic factors must also be considered.<sup>10</sup> The injected fluid must be accommodated by fracture and formation porosity. Depending upon injection rate, fluid viscosity, fracture size, and formation permeability and compressibility some fluid permeates the rock adjacent to the fracture and is thus stored in existing porosity. The remaining fluid is stored in the dilated fracture. In principle, jacking requires higher pressures, which leads to greater dilation than shearing, but rough estimates<sup>11</sup> suggest that formation permeation accommodated 90% of the water injected in these fracturing experiments. Consequently little fracture dilation was required, and despite the vast differences in physical scale this fracturing was probably similar to the shear<sup>12</sup> fracturing observed by Lockner and Byerlee when core specimens were fractured at low injection rates. Thus, it is likely that jacking in the present experiments, if it occurred at all, was confined to low  $\beta$  joints, for which  $S_{min}/P_f \approx 1$ .

To briefly summarize estimated earth stresses at other depths, it is noted that the maximum ratio of  $S_{max}/P_f$  occurs for the biotite granodiorite intrusive, where the ratio is 2, resulting in  $S_{min}/P_f = 1.25 \pm 0.25$  based upon the shear criterion for joints with  $\beta < 45^\circ$ . However in this interval a completed reservoir was developed and simple geometrical relations between fracture initiation zones and intersection zones in the opposite well indicate

nearly vertical fractures,  $\beta < 10^\circ$ , so  $S_{min}/P_f$  is constrained to less than 1.10. The jacking criterion for  $\beta < 10^\circ$  likewise results in  $S_{min}/P_f = 0.95$ . In summary  $S_{min} \approx P_f$  closely for this interval. For depth intervals not yet discussed no similar geometrical constraints are available, but in these intervals  $S_{max}/P_f \approx 1.5$ ; and the shear criterion results in  $S_{min}/P_f = 1.12 \pm 0.12$ .

#### CONCLUSIONS

Fracture pressures were estimated from direct ISIPs, extrapolated ISIPs, observed changes in hydrological characteristics, and extrapolations of fracture extension pressure versus injection rate. Excluding "laminar" flow scaling, and "turbulent" flow scaling where only a very few data sets (P vs Q) are available, excellent agreement is found for all five methods. Because of the nearly lithostatic state of stress at this site, in which the ratio of  $S_{max}/S_{min}$  was typically 1.5 (2.0 in the worst case), it was possible to show that  $S_{min} \approx P_f$  even if the mode of fracturing is shear, or if off-vertical joints were "jacked" open. Except for the Biotite Granodiorite intrusive, where  $S_{min}$  appears to be 20 MPa lower than expected, the minimum principal earth stress is linear with depth, with a gradient of 19 MPa/km (0.84 psi/ft) and is horizontally oriented in approximately the EW direction. The maximum horizontal stress is nearly equal to the overburden stress.

#### REFERENCES

1. Dash, Z., et al, "Hot Dry Rock Geothermal Reservoir Testing: 1978 to 1980", J. Volcan. Geotherm. Res., 15, 59-99, 1983.
2. Aamodt, R. L., and Kuriyagawa, M., "Measurement of Instantaneous Shut-In Pressure in Crystalline Rock", appears in Hydraulic Fracturing Stress Measurements Nat'l Acad. Press Washington, DC, 1983.
3. Perkins, T. K. and Kern, L. R., "Widths of Hydraulic Fractures", J. Petr. Tech., 13, 937-946, September, 1966.
4. Murphy, H. D., Lawton, R. G., Tester, J. W., Potter, R. M., Brown, D. W., and Aamodt, R. L., "Preliminary Assessment of a Geothermal Energy Reservoir Formed by Hydraulic Fracturing", Soc. Petr. Engr. J., 317-326, August 1977.
5. Brown, D. W., "Recent Results - Los Alamos Hot Dry Rock Project", Proc. 8th Workshop Geothermal Reservoir Engineering, Stanford, Univ., December 1982.
6. Pine, R. J. and Batchelor, A. S., "Downward Growth of Hydraulic Stimulation by Shearing in Jointed Rock", submitted to Int. J. Rock Mech. Min. Sci. Geomech Abstr., 1983.
7. Bombolakis, E. G., "Some Constraints and Aids for Interpretation of Fracture and Fault Development", Proc. 2nd Int. Conf. Basement Tectonics, Denver, 1979.
8. Anon. "Differential Strain Curve Analysis and Differential Wave Velocity Analysis of Fenton Hill EE-2 Cores", Dowell Rock Mechanics Laboratory, Tulsa, Oklahoma, November 1983.
9. Cash, D., Homuth, E. F., Keppler, H., Pearson, C., and Sasaki, S., "Fault Plane Solutions for Micro Earthquakes Induced at Fenton Hill Hot Dry Rock Geothermal Site: Implications for the State of Stress Near a Quaternary Volcanic Center", to appear in Geophys. Res. Lett., 1984.
10. Murphy, H. D., Pine, R. J., "Dendritic Hydraulic Fracturing in Geothermal Energy Reservoirs", Proc. Energy Tech. Conf. and Exhibit, New Orleans, Feb. 12-16, 1984.
11. Murphy, H. D. Keppler, H. and Dash, Z., "Does Hydraulic Fracturing Theory Work in Jointed Rock Masses?," Trans. Geotherm. Res. Council 7, 461-466, 1983.
12. Lockner, D. and Byerlee, J. D., "Hydrofracture in Weber Sandstone at High Confining Pressure and Differential Stress", J. Geophys. Res., 82, 2018-2026, 1977.